

Stimulated polariton scattering in intersubband lasers: Role of motional narrowing

J. B. Khurgin

Department of Electrical and Computer Engineering, Johns Hopkins University, Baltimore, Maryland 21218, USA

H. C. Liu

Institute for Microstructural Sciences, National Research Council, Ottawa, Canada K1A 0R6

(Received 20 December 2005; published 14 July 2006)

We have developed a theory of polariton scattering in the inhomogeneously broadened intersubband transitions in multiple quantum wells and showed that motional narrowing plays an important role in the emission of intersubband polaritons. We then analyzed the results of experiments of intersubband Raman lasing in quantum well structures and showed that the lasing process involves stimulated emission of a polariton comprising a photon, an optical phonon, and an intersubband excitation. Our theory offers an explanation for the abnormally high gain of the parametric process in comparison to optically pumped lasers.

DOI: 10.1103/PhysRevB.74.035317

PACS number(s): 71.36.+c, 42.55.Ye, 78.67.De

Since the invention of quantum cascade lasers¹ there has been a keen interest in exploration of various coherent and nonlinear optical phenomena based on the intersubband transitions (ISTs) in quantum wells (QWs). Among these processes are optically pumped intersubband lasing,^{2,3} frequency mixing, and more recently^{4–7} Raman processes. As shown in detail in Ref. 4 there are both similarities and differences between “real” and “virtual” intersubband processes. In the real process—optically pumped lasing [Fig. 1(a)]—an electron population is established in the excited level 3 from which the lasing to the lower state 2 originates. There is no coherence between the pump and laser waves and the frequency of the lasing transition stays constant, $\hbar\omega_{laser}=E_{32}$ independent of the pump detuning $\Delta_{31}=E_{31}-\hbar\omega_p$. In the virtual Raman process the frequency of the emitted Stokes wave follows the pump frequency, $\hbar\omega_s=\hbar\omega_{pump}-E_{21}$ (although the phase of the Stokes wave remains independent of the pump’s phase). According to Ref. 4 the gain of the real process is typically stronger than the Raman one, but the experimental results^{5,7} showed that the frequency of the emitted radiation followed the frequency of the pump with a constant offset—the Stokes shift—a clear indication of a virtual process. That shift, however, was not equal to E_{21} (even with the depolarization shift factored in) indicating that more than a simple intersubband excitation (ISX) was involved.

A more rigorous study⁶ has revealed that the Raman process is strongly affected by the optical phonon resonance, and, in fact, one can consider the lower state a coupled ISX-phonon mode. But these results still did not explain why the Raman process dominates the seemingly more probable real intersubband lasing. Furthermore, the lasing threshold measurements have shown a very strong dependence on the difference between the ISX energy and the Stokes shift (called here the Raman detuning), which has defied explanation. In our opinion, earlier works have not considered important features of optical processes in the three-level IST system. The IST between the lower lasing and ground states is strongly coupled to the optical field; thus in addition to the Raman process there is a fully coherent parametric process in which the pump photon splits into signal and idler photons with full conservation of both energy and momentum as shown in Fig.

1(c). Since the idler wave is strongly coupled to the ISX, one can picture this process as a polariton Raman scattering, which has been observed in Ref. 8, albeit for the case of phonon polaritons in LiNbO₃. A theoretical analysis in Ref. 9 predicted that the maximum gain of the parametric process does not exceed the gain of the normal Raman process due to reabsorption of the idler wave. But that analysis, performed for the phonon polariton, did not account for inhomogeneous broadening, which is very important in ISTs. The broadening is caused by both nonuniformities in the plane of the QWs—“interface islands”¹⁰—and by the thickness variations between different QWs.¹¹

In this paper we show theoretically that when the inhomogeneous broadening is large, the coupling between the ISX, phonons, and photons leads to an increase in the magnitude of parametric gain and explicate this increase as a motional narrowing effect.^{12–14} The developed theory explains the observed threshold dependence on the Raman detuning and thus serves as experimental evidence that the motional narrowing, previously seen only in cavity exciton polaritons at liquid He temperatures, has been observed in the IST medium at elevated (liquid N₂) temperature and without a cavity.

First we set up coupled equations for all the interacting excitations: three electromagnetic waves, pump E_p , signal or Stokes E_s , and idler E_i ; M modes of polarization associated with displacement in M different polar optical phonon modes, $P_{ph,m}$; and the nondiagonal density matrix element

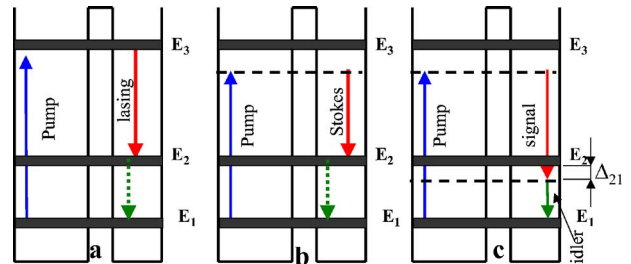


FIG. 1. (Color online) Intersubband processes in a QW. (a) Lasing, (b) stimulated Raman scattering, and (c) parametric down-conversion or stimulated polariton scattering.

ρ_{21} , the collective ISX.^{16,17} The ISTs are subject to both homogeneous broadening described by a Lorentzian shape of linewidth γ_{21} and inhomogeneous broadening described by the deviation from the mean IST energy, $\delta_{21}=E_{21}-\bar{E}_{21}$, with Gaussian distribution $g(\delta_{21})=(2\pi)^{-1/2}\sigma^{-1}\exp(-\delta_{21}^2/2\sigma^2)$. One can introduce the mean one-photon and Raman detunings as $\Delta_{31}=\bar{E}_{31}-\hbar\omega_p$ and $\Delta_{21}=\bar{E}_{21}-\hbar\omega_i$, respectively. We can also introduce the detuning between the idler wave and different optical phonon modes, $\Delta_{LO(TO),m}=E_{LO(TO),m}-\hbar\omega_i$. We assume that the time changes are slow on the scale of the detunings, $\hbar^{-1}\partial/\partial t\ll\sigma, \Delta_{LO,j}, \Delta_{TO,j}$ —thus the polarizations of phonon modes and ISX's follow the fields adiabatically:

$$\frac{\partial^2 E_p}{\partial z^2} - \frac{n_p^2}{c^2} \frac{\partial^2 E_p}{\partial t^2} = \frac{1}{\varepsilon_0 c^2} \int \frac{\partial^2 \rho_{21}(\delta_{21})}{\partial t^2} \frac{N d_{32} d_{31} E_s}{\Delta_{31} - j\gamma_{31}} g(\delta_{21}) d\delta_{21},$$

$$\begin{aligned} \frac{\partial^2 E_s}{\partial z^2} - \frac{n_s^2 \omega_s^2}{c^2} \frac{\partial^2 E_s}{\partial t^2} \\ = \frac{1}{\varepsilon_0 c^2} \int \frac{\partial^2 \rho_{21}^*(\delta_{21})}{\partial t^2} \frac{N d_{32} d_{31} E_p}{\Delta_{31} - j\gamma_{31}} g(\delta_{21}) d\delta_{21}, \end{aligned}$$

$$\begin{aligned} \frac{\partial^2 E_i}{\partial z^2} - \frac{\varepsilon_\infty}{\varepsilon_0 c^2} \frac{\partial^2 E_i}{\partial t^2} \\ = \frac{1}{\varepsilon_0 c^2} \frac{\partial^2}{\partial t^2} \left(\int N \rho_{21}(\delta_{21}) d_{21} g(\delta_{21}) d\delta_{21} + \sum_{m=1}^M P_{ph,m} \right), \end{aligned}$$

$$P_{ph,m} = \varepsilon_\infty \left(\frac{\Delta_{LO,m}^2}{\Delta_{TO,m}^2} - 1 \right) E_i,$$

$$\begin{aligned} \rho_{21}(\delta_{21}) &= \rho_{21}^l + \rho_{21}^R \\ &= \frac{d_{21} E_i}{(\Delta_{21} + \delta_{21} - j\Gamma_{21})} + \frac{d_{32} d_{31} E_p E_s^*}{(\Delta_{31} - j\gamma_{31})(\Delta_{21} + \delta_{21} - j\gamma_{21})}, \end{aligned} \quad (1)$$

where the ISX has both linear ρ_{21}^l and nonlinear (Raman) ρ_{21}^R components. Other parameters are ε_∞ , the background dielectric permittivity, and d_{mn} , the transition dipole matrix elements. The pure phonon Raman contribution is neglected since with both pump and Stokes wave polarized along the [100] direction the bulk Raman tensor is equal to zero.¹⁸ This assumption of mostly an electronic origin of the Raman processes is substantiated also by the fact that no Raman lasing has been observed at large detunings away from the IST energy. The role of the phonons is, nevertheless, crucial to the scattering process discussed here because, as clearly shown below, no momentum conservation (phase matching) can be achieved without phonons.

Next, we can express all the electromagnetic waves as products of slowly varying amplitudes and normalized waveguide modes, $E_q = A_q(z) f_q(x, y) \exp[j\omega_q(n_q z c^{-1} - t)]$, where n_q are the effective refractive indices of the q th mode. We now include the linear part of the IST and phonon polarizations into the expression for the effective refractive index of the idler wave and obtain

$$\begin{aligned} \frac{dA_i}{dz} &= j \frac{\omega_i N d_{21} d_{32} d_{31} A_p A_s^*}{2n_i \varepsilon_0 c} \Gamma_{ips} \int \frac{g(\delta'_{21}) d\delta'_{21}}{\Delta_{31}(\Delta_{21} + \delta'_{21} - j\gamma_{21})} \\ &\quad - \frac{\omega_i N d_{21}^2 A_i}{2n_i \varepsilon_0 c} \Gamma_{ii} \int \frac{\gamma_{21} g(\delta'_{21}) d\delta'_{21}}{(\Delta_{21} + \delta'_{21})^2 + \gamma_{21}^2} - \frac{\omega_i}{2n_i c} \chi'' A_i, \end{aligned} \quad (2)$$

where the mode overlaps are $\Gamma_{qlm} = \int \int f_q f_l f_m(x, y) Q(x, y) dx dy$, and $Q(x, y)$ is the function indicating the transverse distribution of the QW's. The first term in Eq. (2) is a two-photon (Raman) driver, the second one is the loss due to reabsorption by the IST, and the third term is the loss due to scattering and diffraction, expressed here in units of susceptibility. The idler frequency is determined from phase matching $\omega_i n_i = \omega_p n_p - \omega_s n_s$ to be discussed later. Here we assumed, for simplicity, $\Delta_{31} \gg \gamma_{31}$. Our full numerical results show that keeping the γ_{31} term does not alter the main conclusions of our work and only amounts to a decrease of nonlinearity due to pump absorption. Solving Eq. (2) for the steady-state value of the idler, substituting it into Eq. (1), and performing integration over the transverse mode distribution, we obtain

$$\begin{aligned} \frac{dA_s}{dz} &= j \frac{\omega_i d_{13}^2 |A_p|^2 A_s}{2n_i c \Delta_{31}^2} \chi^*(\Delta_{21}) \\ &\quad \times \left[\frac{|\Gamma_{ips}|^2}{\Gamma_{ii}} \left(j \frac{\chi_r(\Delta_{21})}{\chi_i(\Delta_{21})} - 1 \right) F(\Delta_{21}) + \Gamma_{ppss} \right] \end{aligned} \quad (3)$$

where $\chi(\Delta_{21}) = (N d_{21}^2 / \varepsilon_0) \int [g(\delta'_{21}) d\delta'_{21} / (\Delta_{21} + \delta'_{21} - j\gamma_{21})]$ is the IST susceptibility and $\chi_r(\Delta_{21})$ and $\chi_i(\Delta_{21})$ are its real and imaginary parts, and the relative strength of the IST-photon coupling $F(\Delta_{21}) = \chi_i(\Delta_{21}) / [\chi_i(\Delta_{21}) + \chi'']$ varies from 1 in the absence of additional loss to 0. One can see that the main impact of the IST coupling to the photon and back is the $\pi/2$ phase shift; hence, unlike the pure Raman gain, the parametric gain does not exhibit sharp resonances associated with the absorptive part of the susceptibility. This leads to important consequences as we obtain the expression for the total gain at the signal frequency as a sum of parametric and Raman gains

$$\begin{aligned} G(\Delta_{21}) &= G_p(\Delta_{21}) + G_R(\Delta_{21}) \\ &= G_0 \frac{|\Gamma_{ips}|^2}{\Gamma_{ii}} \left[F(\Delta_{21}) C_P(\Delta_{21}) \right. \\ &\quad \left. + \left(\frac{\Gamma_{ppss} \Gamma_{ii}}{|\Gamma_{ips}|^2} - F(\Delta_{21}) \right) C_R(\Delta_{21}) \right] \end{aligned} \quad (4)$$

where $G_0 = \omega_i N d_{13}^2 d_{21}^2 |A_p|^2 / 2n_i \varepsilon_0 c \Delta_{31}^2$, and the shapes for parametric and Raman components are

$$C_P(\Delta_{21}) = \frac{\gamma_{21} \varepsilon_0 \chi_r^2(\Delta_{21})}{N d_{21}^2 \chi_i(\Delta_{21})}, \quad C_R(\Delta_{21}) = \frac{\gamma_{21} \varepsilon_0}{N d_{21}^2} \chi_i(\Delta_{21}). \quad (5)$$

The shapes are plotted in Fig. 2 for the case of linewidth ratio $\sigma/\gamma_{21}=4$. The pure Raman gain is a Voigt shape with maximum at $\Delta_{21}=0$ that is equal to $C_R(0) \sim \sqrt{\pi/2} \gamma_{21}/\sigma$, which is easy to interpret—only a small resonant fraction of ISTs participate in the Raman process. The parametric shape, on the other hand, shows the opposite trend, increasing from

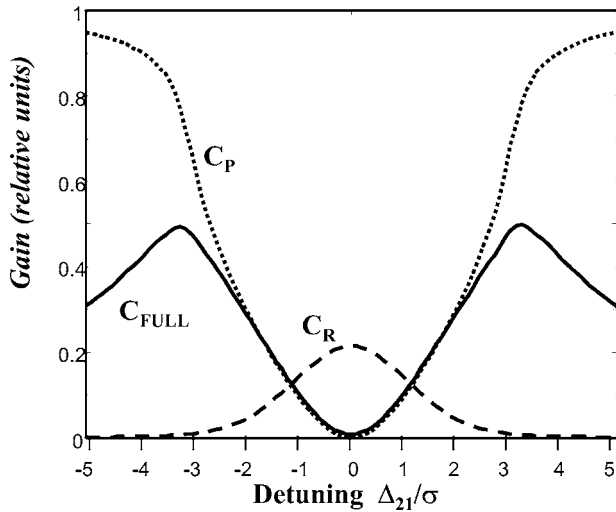


FIG. 2. Gain shape factors for ideal Raman (C_R) process, ideal Polariton scattering (C_P) and complete gain in the presence of non-resonant loss (C_{full}).

zero at $\Delta_{21}=0$ to nearly unity at large detunings, where reduction

in strength of the photon-IST coupling is more than balanced by the decrease of reabsorption by the IST. Thus maximum parametric gain is achieved away from the resonance with the central IST frequency as is expected for the polariton effect. However, at large detunings the presence of other loss mechanisms [$F(\Delta_{21}) < 1$] reduces actual parametric gain—this is also shown in Fig. 2 where we have plotted the complete gain shape $C_{full}(\Delta_{21}) = F(\Delta_{21})C_P(\Delta_{21}) + [1 - F(\Delta_{21})]C_R(\Delta_{21})$ assuming the nonresonant loss to be 10% of the peak IST absorption ($\chi'' = 0.1\chi_I$).

The semiclassical analysis performed here shows that for the inhomogeneous transitions the strength of stimulated scattering is increased by about σ/γ_{21} . This conclusion is quite different from the prior work of Henry and Garrett⁹ who dealt with phonon-polaritons and did not consider the inhomogeneous broadening. Our results can be most clearly interpreted as the effect of motional narrowing occurring when the particle moving rapidly in the nonuniform environment tends to average the potential fluctuations occurring on a relatively small spatial scale. Motional narrowing plays the most prominent role in the NMR,¹⁹ but more recently had been discovered for the case of cavity exciton-polaritons.^{12–15} For the case of ISTs one can understand motional narrowing as follows: in the absence of coupling to the electromagnetic waves the single-particle ISXs are localized on the nonuniformities of the QW's.^{10,11} When the ISX and the nearly zero-effective-mass photon are coupled into a polariton, as shown in Fig. 3(a), the polariton gets delocalized (as is evidenced by the nonzero group velocity) and does not see the small-scale potential fluctuations. Thus all the ISTs get involved in the polariton-related scattering, rather than only a small fraction γ_{21}/σ accessible via the pure Raman process. It is also clear that the further away the polariton gets from the IST resonance, the larger is its group velocity and thus the more prominent becomes the effect of motional narrowing—in perfect agreement with Fig. 2 based on the semiclassical derivation.

We now return to the important role played by phonons. In order to obtain the actual polariton frequency ω_i one needs to find the intersection of the polariton dispersion curve $\omega_i(\beta)$ shown in Fig. 3(a) with the phase-matching curve $\beta = c^{-1}[\omega_p(n_p - n_s) + \omega_i n_s]$. In the absence of phonons the dispersion is normal, $n_p \sim n_s > n_i$, and the phase-matching condition can only be satisfied for the lower polariton branch. In the experiment,^{5,6} however, the lasing has always taken place at negative values of Δ_{21} , i.e., involving the upper polariton branch. This can be explained by the fact that in the vicinity of resonance with optical phonons the dispersion is anomalous and more than one polariton branch can be phase matched to the ISX wave. Thus the polariton produced by resonant scattering contains in addition to ISX and photon components contributions from one or more phonon branches. In the literature, collective ISX is often referred to as an intersubband plasmon—thus the quasiparticle considered here can be called an intersubband plasmon-phonon-polariton, or IP³.

In Figs. 3(b)–3(d) we show the dispersion curves of IP³ in the vicinity of resonance with the confined optical phonons of GaAs and AlAs as well as with one interface mode for three different values of IST energies. These curves are obtained by solving a set of coupled equations similar to (1). Since three phonon branches are involved in the IP³, the curve has five branches, four of which at some point intersect with the two-photon excitation dispersion line. However, according to Fig. 2 only for the branches that are reasonably close to IST is the gain sufficiently strong to initiate the stimulated scattering process observed in experiments. The interplay between gain and loss determines which mode will oscillate. When two IP³ modes have stimulated scattering gains that are close to each other, a small change in the IST energy can cause the parametric process to switch between two modes, as can be seen by comparing Figs. 3(c) and 3(d). Although the higher-energy polariton associated with the interface mode in Fig. 3(d) is further from the IST resonance than the GaAs polariton, the overall scattering gain in it is larger as in Fig. 2 so it is the higher-energy polariton that oscillates. Indeed such sharp changes in the Stokes shift were observed in experiments. Using the IP³ theory derived here one can obtain very good agreement between the Stokes shift and IST energy; however, such agreement in itself is not a definite proof of the polariton character of the scattering—similar agreement has been obtained by considering only two coupled entities, the intersubband plasmon and the LO phonon. This is of course no wonder since the coupled-mode theory is nothing but the unretarded approximation of IP³ theory; thus when it comes to the eigenenergies the results are quite similar. In the unretarded approximation the field does not propagate and thus ISX–LO-phonon coupling takes place on the local scale and the energy spectrum of the combined quasiparticles still has the original IST broadening σ with no motional narrowing effect on gain. If anything, one would expect the gain to decrease with increase in Δ_{21} . To check the assumption of whether the lasing is based on Raman scattering of the combined ISX–LO-phonon particle or the process is an IP³ (parametric) scattering, one must investigate the gain, or the laser threshold, as a function of Raman detuning.

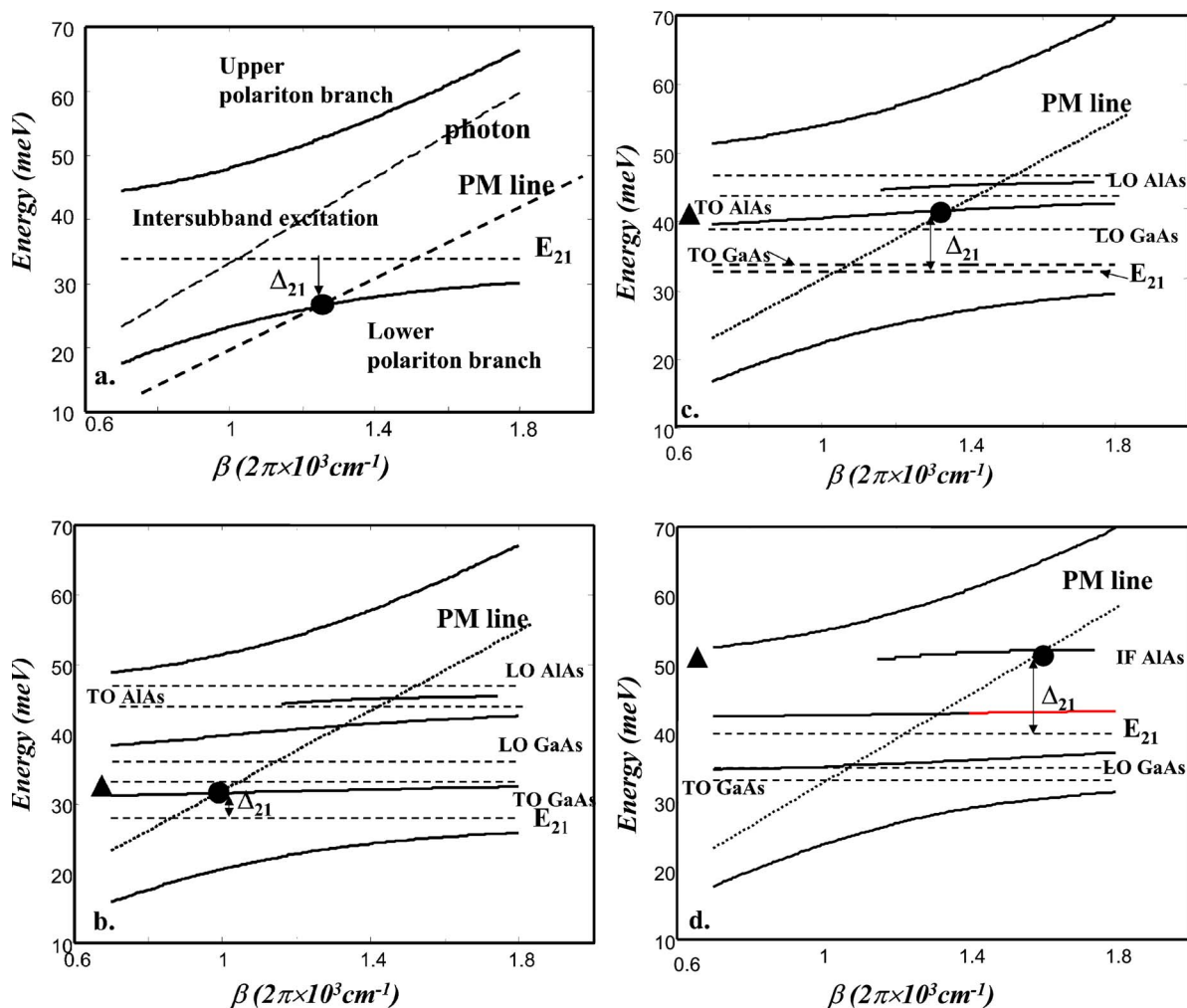


FIG. 3. (Color online) (a) Dispersion curve of intersubband polariton and phase-matching (PM) curve in the absence of phonons. (b)–(d) Dispersion curves for the intersubband plasmon-phonon-polariton (IP³) for different values of the IST energy E_{21} . Solid circles indicate the energy and momentum of the emitted IP³ determined by phase matching, and triangles indicate measured Stokes shift. Dashed lines are the energies of longitudinal optical (LO), transverse optical (TO), and interface (IF) phonons.

In Fig. 4 we have plotted lasing thresholds of different samples versus Raman detuning. The samples are the same as in Ref. 6, where experimental details are given. We stress that the measurement error in the determination of the threshold is small (within $\pm 5\%$). The main error relates to the quality difference among different wafers. We are, however, confident that the sample difference is quite small as evidenced by the very similar IST linewidths directly observed in transmission and absorption measurements. We then plotted the function $[C_{full}(\Delta_{21})]^{-1}$ using the experimentally measured value of inhomogeneous broadening $\sigma \sim 3.5$ meV (full width at half maximum ~ 9 meV). As far as γ_{21} is concerned, its value is difficult to ascertain but it can be safely assumed to be low. The strongest interaction capable of scattering the collective ISX, that with the LO phonon, is already factored into the coupling Hamiltonian—thus the only remaining causes for coupled ISX scattering are the interactions with single-particle intersubband excitations and the anharmonic decay of the phonon.^{20,21} In our calculation we assume $\gamma_{21} \sim 1$ meV. As one can see, a reasonable fit to experimental data is obtained. Since to the best of our knowl-

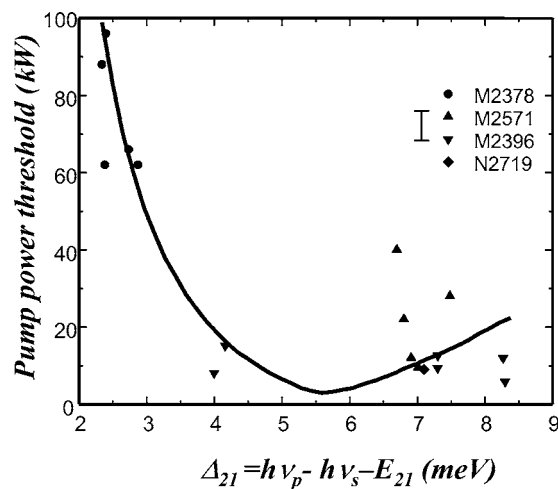


FIG. 4. Lasing threshold of the intersubband emitter of Fig. 1 vs Raman detuning. Points, experimental data; solid line, theoretical curve.

edge such a strong and counterintuitive dependence of lasing threshold on detuning cannot be explained in the framework of either optically pumped or conventional Raman lasing, this fit in our opinion serves as unambiguous proof of the polariton character of the observed Raman lasing and motional narrowing associated with it.

In conclusion we have developed a theory of polariton scattering in the inhomogeneously broadened IST in the vicinity of phonon resonance and have shown that motional

narrowing plays an important role in the emission of inter-subband polaritons. Our theory offers an explanation for the abnormally high gain of the parametric process in comparison to optically pumped lasers.

We thank C. Y. Song and I. W. Cheung for infrared measurements, and Z. R. Wasilewski and A. J. SpringThorpe for materials growth.

-
- ¹J. Faist, F. Capasso, D. L. Sivco, C. Sirtori, A. L. Hutchinson, and A. Y. Cho, *Science* **254**, 553 (1994).
- ²G. Sun and J. B. Khurgin, *IEEE J. Quantum Electron.* **29**, 1104 (1993).
- ³O. Gauthier-Lafaye, F. H. Julien, S. Cabaret, J. M. Laurite, G. Strasser, E. Gornik, M. Helm, and P. Bois, *Appl. Phys. Lett.* **74**, 1537 (1999).
- ⁴J. B. Khurgin and G. Sun, *J. Appl. Phys.* **78**, 7398 (1995).
- ⁵H. C. Liu, I. W. Cheung, A. J. SpringThorpe, C. Dharma-wardana, Z. R. Wasilewski, G. C. Aers, and D. J. Lockwood, *Appl. Phys. Lett.* **78**, 3580 (2001).
- ⁶H. C. Liu, C. Y. Song, Z. R. Wasilewski, A. J. SpringThorpe, J. C. Cao, C. Dharma-Wardana, G. C. Aers, D. J. Lockwood, and J. A. Gupta, *Phys. Rev. Lett.* **90**, 077402 (2003).
- ⁷M. Troccoli, A. Belyanin, F. Capasso, E. Cubukcu, D. L. Sivco, and A. Y. Cho, *Nature (London)* **433**, 845 (2005).
- ⁸J. M. Yarborough, S. S. Sussman, H. E. Puthoff, R. H. Pantell, and B. C. Johnson, *Appl. Phys. Lett.* **15**, 102 (1969).
- ⁹C. H. Henry and C. G. B. Garrett, *Phys. Rev.* **171**, 1058 (1968).
- ¹⁰M. Jaros and A. W. Beavis, *Appl. Phys. Lett.* **63**, 669 (1993).
- ¹¹Y. J. Ding, D. C. Reynolds, S. J. Lee, J. B. Khurgin, W. S. Rabinovioch, and D. S. Katzer, *Appl. Phys. Lett.* **71**, 2581 (1997).
- ¹²D. M. Whittaker, P. Kinsler, T. A. Fisher, M. S. Skolnick, A. Armitage, A. M. Afshar, M. D. Sturge, and J. S. Roberts, *Phys. Rev. Lett.* **77**, 4792 (1996).
- ¹³M. S. Skolnick, T. A. Fisher, and D. M. Whittaker, *Semicond. Sci. Technol.* **13**, 645 (1998).
- ¹⁴D. M. Whittaker, *Phys. Rev. Lett.* **80**, 4791 (1998).
- ¹⁵J. J. Baumberg, A. P. Heberle, A. V. Kavokin, M. R. Vladimirova, and K. Kohler, *Phys. Rev. Lett.* **80**, 3567 (1998).
- ¹⁶D. Marcuse, *Principles of Quantum Electronics* (Academic Press, New York, 1980).
- ¹⁷M. Born and K. Huang, *Dynamical Theory of Crystal Lattices* (Oxford University Press, New York, 1988).
- ¹⁸P. Y. Yu and M. Cardona, *Fundamentals of Semiconductors* (Springer, Berlin, 1995), p. 367.
- ¹⁹D. Craik, *Magnetism: Principles and Applications* (Wiley, New York, 1995), pp. 240–245.
- ²⁰P. G. Klemens, *Phys. Rev.* **148**, 845 (1966).
- ²¹A. Debernardi, *Phys. Rev. B* **57**, 12847 (1998).